# Tunable Energy Release in a Reversible Molecular Solar Thermal System

Evanie Franz[a], Corinna Stumm[a], Fabian Waidhas[a], Manon Bertram[a], Martyn Jevric[b], Jessica Orrego-Hernadez[b], Helen Hölzel[b], Kasper Moth-Poulsen[b,c,d], Olaf Brummel[a]*, Jörg Libuda[a]

[a] Interface Research and Catalysis, ECRC, Friedrich-Alexander-Universität Erlangen-Nürnberg, Egerlandstraße 3, 91058 Erlangen, Germany
[b] Chalmers University of Technology, Kemivägen 4, Gothenburg, 41296, Sweden
[c] The Institute of Materials Science of Barcelona, ICMAB-CSIC, 08193 Bellaterra, Barcelona, Spain
[d] Catalan Institution for Research & Advanced Studies, ICREA, Pg. Lluís Companys 23, Barcelona, Spain
*corresponding author: Olaf Brummel olaf.brummel@fau.de

KEYWORDS: Energy Storage, Photoswitches, Norbornadiene, Quadricyclane, Gold, Heterogeneous Catalysis, Solar Thermal Fuels

**Abstract**

Molecular solar thermal (MOST) systems open application fields for solar energy conversion, as they combine conversion, storage, and release in one single molecule. For the energy release, catalysts must be controllable, selective, and stable over many operation cycles. Here, we present a MOST/catalyst couple, which combines all these properties. We explore solar energy storage in a tailor-made MOST system (cyano-3-(3,4-dimethoxyphenyl)-norbornadiene/quadricyclane; NBD'/QC') and the energy release heterogeneously catalyzed at a Au(111) surface. By photoelectrochemical infrared reflection absorption spectroscopy (PEC-IRRAS) and scanning tunneling microscopy (STM), we show that Au triggers the energy release with very high activity. Most remarkably, the release rate of the heterogeneously catalyzed process can be tuned by applying an external potential. Our durability tests show that the MOST/catalyst system is stable over 1000 storage cycles without any decomposition. The surface structure of the catalyst is preserved and its activity decreases by only 0.1% per storage cycle.

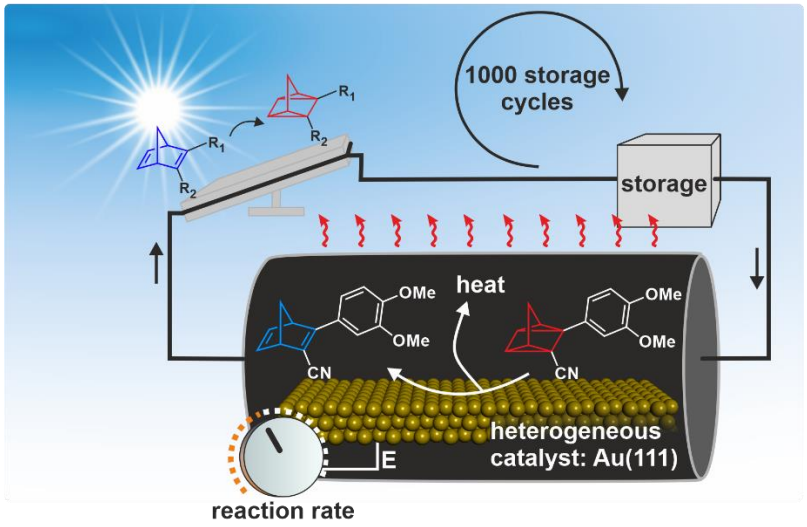


**TOC Figure only.**

## Introduction

For the transition to a sustainable energy system, it is essential to harvest and store solar energy in various ways. Besides established approaches, such as photovoltaics combined with batteries or power-to-X technologies, smart molecular concepts may provide simple, small-scale solutions with the potential to complement the portfolio of established technologies for specific applications. In this context, a particular promising concept is the storage of solar energy in so-called molecular solar thermal (MOST) systems.[1-4] Here, molecular switches are used which photoisomerize to a high-energy metastable state upon exposure to sunlight.[4, 5] Several different classes of molecules have been used in MOST systems,[4-7] for example azobenzenes,[8, 9] dihydroazulenes,[10] and 1,2-azaborines[11]. One of the most prominent examples in this field is the valence isomer pair of norbornadiene (NBD) and quadricyclane (QC).[12-14] Here the parent molecule NBD is converted photochemically to its energy-rich photoisomer QC via an intramolecular [2+2] cycloaddition. The stored energy can be released at will, which implies that the photoswitch combines conversion and storage functionalities in a single molecule.[15] The NBD/QC storage couple has recently received particular attention[16-19] because its energy storage capacity may be as large as 100 kJ $mol^{-1}$ (1 $MJ \cdot kg^{-1}$).[4, 14, 20] This value implies that energy densities could be achieved that are comparable to those of state-of-the-art Li-ion batteries.[21] Note that high energy densities are advantageous for both stationary and non-stationary applications. With a NBD/QC derivative similar to the one used in this study, some of the authors reached an increase of temperature of 63 K during the back-conversion.[22] MOSTs can be coupled with other technologies in hybrid systems, such as MOST water heating hybrid systems,[23] MOST phase-change material hybrid systems,[24] and MOST-thermoelectric generator (TEG) systems for electric power generation.[25] For a detailed description of the metrics and applications of MOSTs we refer to our recently published review article.[4]

Still, there are major challenges that must be addressed to make MOST technology applicable in devices.[4, 14, 20, 25-31] A particular demanding challenge is to control the energy release process in a reliable fashion. Common procedures to trigger the back-conversion rely on the addition of homogenous, mildly oxidizing agents[32-34]. Commonly used heterogeneous catalysts are supported cobalt(II) porphyrin derivatives,[35, 36] copper(II) and tin(II) salts,[37] metal oxides,[38] and cobalt(II) complexes.[39] Fascinatingly, it has also been demonstrated that gold has a remarkable influence on the photochemical properties of molecular switches.[40, 41] Recently, Herges and coworkers showed that Au triggers the back-conversion in azobenzene photoswitches and proposed a singlet–triplet–

singlet spin change mechanism.[42] In a very recent surface science study, we were able to demonstrate that Au also catalyzes the energy release from tailor-made NBD derivatives, directly linked to the Au surface.[43, 44]

For practical applications, it would be most convenient to release the energy from MOSTs via a heterogeneously catalyzed process in a flow reactor, because this would enable catalyst separation, adjustable energy release, and a straightforward path for implementation into larger devices.[35, 45] Also, the electrochemically triggered energy release, which follows a different reaction channel (see Supporting Information Chapter 8 for details), provides some practical advantages such as straightforward control over the release rate via the potential applied.[29, 46-48]

In this work, we combine the best of both worlds, i.e. heterogeneous catalysis (reaction channel) and electrochemistry (controllability). We use an Au electrode, which shows very high catalytic activity, while the rate of this heterogeneously catalysed reaction can still be tuned via the electrode potential. In other words, we can switch on and off the catalytic channel via the potential applied. In this way, we design a 'catalytic valve' for the MOST/catalyst system that combines extremely high reversibility, very high activity, and easy switchability. In specific, we investigated the NBD derivative cyano-3-(3,4-dimethoxyphenyl)-NBD (NBD') and its photochemical conversion to the corresponding QC derivative (QC'). The energy release was triggered catalytically by Au(111) at the solid/liquid interface. We monitored the reaction in-situ by photoelectrochemical infrared reflection absorption spectroscopy (PEC-IRRAS) and investigated the structure of the catalyst surface by scanning tunneling microscopy (STM). We demonstrate that the Au(111) surface shows high catalytic activity, selectivity, and stability, and the storage system remains operational over more than 1000 storage cycles. Most fascinatingly, we show that we can control the energy release rate of the heterogeneously catalyzed reaction pathway by an externally applied potential.

**Results and Discussion**

The MOST/catalyst couple cyano-3-(3,4-dimethoxyphenyl)-NBD/QC (NBD'/QC') studied in this work is depicted in Figure 1. NBD' has the absorption maximum $\lambda_{max}$(NBD') at 340 nm, the absorption onset $\lambda_{onset}$(NBD') at 389 nm and converts into QC' with an quantum efficiency $\Phi$ of 68%.[49] In the experiment NBD' is photoconverted in solution to QC' and, subsequently, NBD' is back-converted catalytically at a Au(111) single crystal surface. In a first step, we investigated the energy storage and release reaction in-situ by PEC-IRRAS. We used a tailor-made setup

schematically depicted in **Figure 1** (see Brummel et al.[29] and Methods). During the measurements, the Au(111) sample was pressed against a $CaF_2$ window with a Teflon spacer of 25 µm generating a thin layer of NBD/electrolyte solution. Note that in this thin-layer configuration the reactant exchange between the thin-layer and the bulk solution is suppressed (see Supporting Information for details). The thin layer was irradiated by an UV LED placed underneath the $CaF_2$ window. In a first step, we investigated the photochemical conversion of a 10 mM solution of NBD' in MeCN and the subsequent back-conversion of QC'. Time-resolved IR spectra were recorded permanently during and after the irradiation. In addition, we performed the experiment with different external potentials applied to the Au electrode. The complete IR spectra between 1100 and 2500 $cm^{-1}$ are shown in **Figure SI 1** in the Supporting Information. Here, we focus on the ν(CN) region only, which allows us to monitor the conversion between NBD' and QC' in a straightforward fashion. An exemplary set of data recorded at an electrode potential of -0.7 $V_{fc}$ is shown in **Figure 2**. Upon conversion to QC', the ν(CN) mode of NBD' blue-shifts by ~25 $cm^{-1}$. We use this frequency shift as a spectroscopic fingerprint enabling straightforward identification of the isomers.[47, 48] As we measure difference spectra, positive (blue) bands correspond to species that are consumed while negative (red) bands are related to the formation of a species. Accordingly, the positive ν(CN) bands of NBD' at 2195 $cm^{-1}$ and the negative ν(CN) bands of QC' at 2219 $cm^{-1}$, which appear upon irradiation, indicate the photochemical conversion of NBD' to QC'. After switching off the UV light, the peaks of the NBD' and QC' modes decay within seconds, indicating fast catalytic back-conversion of QC' to NBD'. Note that the metastable QC' in the absence of a catalyst has a half-life time of 29 days[35], is reductively stable down to 2.0 $V_{fc}$ (see Chapter 9 in the Supporting Information) and the oxidative reaction channel triggered electrochemically occurs at much higher potentials (>0.0 $V_{fc}$).[47, 48] Therefore, the experiment clearly demonstrates that the Au surface is highly active for the catalytically triggered back-conversion of QC' to NBD'. In a recent study, we showed that the catalytic back-conversion requires direct electronic contact with the Au.[44] This observation is compatible with the singlet-triplet mechanism proposed previously by Herges, Tuczek, Magnussen and coworkers, which differs significantly from the radical chain mechanism in the electrocatalytic reaction channel.[42]

From the band intensities, we can derive the concentration of NBD' and QC' as a function of time (see Supporting Information for details). In **Figure 2b**, we depict the corresponding data, both during the photochemical conversion and the catalytically triggered back-conversion. We observe

that during irradiation a steady-state is rapidly established ($t_{1/2}$ = 0.5 s) in which approximately 50% of the photoswitch is present in the form of QC' and 50% in the form of NBD' (due to rapid back conversion at the Au surface). Note that we demonstrated in previous work that total photochemical conversion is possible using catalytically inactive electrode material.[48] After switching off the UV light, QC' is rapidly back-converted to NBD'.

To quantify the rate of the catalytic back-transformation, we developed a kinetic model which we describe in the Supporting Information (see Chapter 3 Supporting Information). For the data shown in **Figure 2b**, we obtain a rate constant of $k_s = 5.6 \cdot 10^{-6}$ m·s$^{-1}$ for the surface reaction. To put this value into context, we compared the rate constants for the back-conversion on Au(111) and Pt(111) under identical conditions (see Supporting Information Chapter 7 for details). Note that Pt(111) is a very active catalyst for the back-conversion reaction.[15] The activity of Au(111), however, exceeds the catalytic activity of Pt(111) by more than 200 times. A possible explanation is a higher resistance of Au(111) against poisoning.

Furthermore, we did not observe any bands in the IR spectra, which would indicate the formation of side products. This observation shows that the photochemical conversion and the catalytically triggered back-conversion are fully reversible within the accuracy of our experiment.

In the next step, we explored whether it is possible to control the kinetics of the heterogeneously catalyzed reaction channel via the externally applied potential. To this aim, we measured the catalytic activity of Au(111) for the back-conversion reaction at potentials between -0.3 $V_{fc}$ and -1.0 $V_{fc}$. In **Figure 3**, we depict the corresponding changes in the concentration of NBD' and QC'. In line with the previous experiment, QC' is formed during irradiation and back-converts to NBD' after switching off the UV light. We observe that the steady-state concentration of QC' increases with decreasing potential while the time constant for the back-conversion decreases. This observation clearly shows that the potential applied to the Au electrode directly affects the rate of the catalytically triggered back-conversion reaction. Here, it is very important to note that the oxidatively triggered back-reaction occurs at much higher potentials (>0.0 $V_{fc}$).[48] A detailed discussion of the potential region is provided in the Supporting Information. This shows that we are not dealing with an electrochemically triggered reaction but are in a purely catalytic regime. In other words, the rate of the heterogeneously catalyzed process depends on the electrical potential applied. Note that the behavior is fully reversible when the potential returns to its original value (see also Chapter 4.1 Supporting Information).

To quantify the effect of the electrode potential on the reaction rate, we determined the rate constants for the catalytic surface reaction $k_s$ as a function of the potential applied (**Figure 4**). Details on the analysis procedure are provided in the Supporting Information. When changing the potential of the Au catalyst from -0.3 to -1.0 $V_{fc}$, the rate constant for the catalytically triggered energy release decreases by a factor of nearly 60, i.e. from $5.7 \cdot 10^{-5}$ to $1.0 \cdot 10^{-6}$ $m \cdot s^{-1}$. We also measured the rate constant in the absence of any externally applied potential (open circuit potential, OCP) to be $2 \cdot 10^{-4}$ $m \cdot s^{-1}$ (see Chapter 7, Supporting Information). Our observations show that the catalytic activity of the Au catalyst can be tuned by an externally applied potential over more than two orders of magnitude.

In other words, the Au surface serves as a 'catalytic valve', which can be opened and closed via the potential. This surprising finding opens a completely new and quite easy to implement pathway for controlling the energy release rate from the catalytic MOST reactor. We propose that the effect originates from the electronic contact of the QC' with the Au catalyst[44], which changes as a function of the potential applied, e.g. due to potential dependent adsorption of ions (i.e. blocking of active sites), potential dependent orientation of the reactants or potential dependent changes of the electronic structure.

In the last step, we scrutinized the stability of the MOST/catalyst system over extended operating periods. To this aim, we studied the photochemical conversion and the catalytically triggered energy release in-situ for 1000 storage and release cycles. The stability experiments were performed under potential control and at OCP (see Chapter 6 of the Supporting Information). The corresponding data for an electrode potential of -0.7 $V_{fc}$ is shown in **Figures 5a** and **5b**. We observe that the MOST/catalyst couple remains operational over the full duration of 1000 storage cycles. We observe only a small increase in the steady-state concentration of QC', which indicates a small decrease in the catalytic reaction rate. In order to quantify the effect, we calculated the corresponding rate constant using the kinetic model described in the Supporting Information. We find that the rate constant for the catalytically triggered energy release $k_s$ decreases by approximately a factor of 4 over 1000 storage cycles (from $6.0 \cdot 10^{-5}$ $m \cdot s^{-1}$ to $1.6 \cdot 10^{-5}$ $m \cdot s^{-1}$, see **Figure 5b**). This implies that the rate constant decreases by only 0.1% per storage cycle and is still very high even after 1000 storage cycles.

This is in sharp contrast to other catalytically active surfaces, for which the reaction rate typically drops by several orders of magnitude.[47] Very importantly, the QC' is always fully back-converted

to NBD' on Au(111) for 1000 cycles, which means that there is no indication for decomposition of NBD' over the full duration of the experiment.

We also investigated the stability of the Au(111) surface under reaction conditions. To this aim, we irradiated freshly prepared Au(111) surfaces for 60 minutes continuously in (i) the pure solvent MeCN and in (ii) a 10 mM NBD' solution at OCP. After rinsing the surfaces, we studied the morphology of the Au(111) catalyst by STM. The corresponding images are shown in **Figures 5c** and **d**, respectively. In both cases, we observe large flat terraces with sharp step edges as expected for well-ordered Au(111). Small islands with a height of 2.2 to 2.6 Å on the surface irradiated in the presence of NBD' we assign to residues of the photoswitch, which remain adsorbed after the rinsing. Most importantly, we do not observe the formation of holes or roughening of the step edges. This observation shows that there is no dissolution or etching during operation, i.e. the surface of the Au(111) catalyst is perfectly stable under experimental conditions.

**Conclusion**

We studied the energy release in the MOST system 2-cyano-3-(3,4-dimethoxyphenyl)-NBD/QC using Au(111) as catalyst. By in-situ photoelectrochemical IR spectroscopy and STM, we investigated the catalytic activity of the Au(111) surface, the influence of an externally applied potential on the reaction kinetics, the reversibility of the system over extended operation periods, and the stability of the catalyst surface. From our findings we conclude the following:

*Catalytic activity:* Au(111) exhibits very high catalytic activity for the back-conversion from QC' to NBD'. The highest rate constants measured for the catalytically triggered back-reaction were in the order of $k_s = 2 \cdot 10^{-4}$ m·s$^{-1}$ at OCP, which exceeds the reaction rates on the highly active Pt(111) surface under identical conditions by more than two orders of magnitude.

*Modification of the catalytic activity by an externally applied potential:* It is possible to tune the kinetics of the heterogeneously catalyzed energy release reaction by an externally applied potential. The rate constant for the catalytic reaction channel decreases by a factor of 60 when the electrode potential decreases from -0.3 to -1.0 $V_{fc}$. With respect to OCP, the rate can be suppressed by more than two orders of magnitude. This effect allows us to build a 'catalytic valve', which can be opened and closed via the potential applied.

*Catalysts stability:* There are no morphological changes of the Au(111) catalyst upon irradiation in the presence of solvent and NBD', indicating that there is no etching or corrosion of the surface.

After 1000 storage and release cycles, the MOST/catalyst system remains fully operational. The rate constant for the catalytically triggered reaction decreases by a factor of 4, which implies that the rate constant decreases by only 0.1% per storage cycle.

*Reversibility:* No side products or decomposition of NBD' or QC' were detected even after 1000 storage and release cycles, both under potential control and at OCP.

Our results show that the here proposed MOST/catalyst couple provides an exceptional combination of properties. The Au(111) surface shows very high catalytic activity and stability, even at extended operation periods. Most importantly, our results show that catalytic activity can be controlled by applying an external potential. This shall enable us to build 'catalytic valves', which will allow us to control the energy release rate in future MOST devices in a very simple and straightforward fashion.

**Methods:**

**Synthesis of 2-cyano-3-(3,4-dimethoxyphenyl)norbornadiene (NBD'):** Cyclopentadiene (7 mL, 83 mM), 3-(3,4-dimethoxyphenyl)propiolonitrile (6.31 g, 33.7 mM), butylated hydroxytoluene (20 mg) and chlorobenzene (7 mL) were heated in a sealed vial to 403 K for 20 h using a microwave reactor. The mixture was purified using flash column chromatography ($CH_2Cl_2$) and recrystallization ($Et_2O$/n-heptane 255 K) to give NBD' as a white crystalline powder (yield: 6.83 g, 80%). For further details on the synthesis, we refer to literature.[31]

**Cleaning of the equipment:** All glass and Teflon ware as well as all noble metal wires, which were used in the in-situ measurements, were stored in a solution of NOCHROMIX® (Sigma Aldrich) in concentrated sulfuric acid (Merck, Emsure, 98%). Prior to each experiment, the equipment was rinsed 5 times with ultra-pure water (MilliQ Synergy UV, 18.2 MΩ·cm at 298 K, TOC < 5 ppm) and subsequently boiled 3 times in Milli-Q water for at least 15 min. Finally, the equipment was dried under reduced pressure overnight.

**PEC-IRRAS:** All infrared spectra were recorded using a vacuum-based Fourier-transform infrared (FT-IR) spectrometer (Bruker, Vertex 80v) with evacuated optics and a liquid-nitrogen-cooled mercury cadmium telluride (MCT) detector. Time-resolved spectra were recorded with a scanner velocity of 240 kHz and a resolution of 8 $cm^{-1}$ leading to an acquisition time of 42 ms per spectrum. For the photochemical measurements, the setup was equipped with a UV LED (Seoul Viosys, CUD4AF1B, 340 nm, 55 mW) underneath a $CaF_2$ hemisphere (Korth, d = 25 mm), which

serves as IR and UV transparent window. As the detector is sensitive to UV light, it was protected by an additional KRS-5 filter. For details on the PEC-IRRAS setup we refer to our previous work.[29, 50]

The Au(111) single crystal (MaTeck, 99.999%, d = 10 mm, roughness < 10 nm, accuracy < 0.1°) was prepared by inductive heating (Ambrell, EasyHeat) at 873 – 1073 K for 30 min. The measurements were performed in reflection mode, using a thin layer configuration. In all experiments, a solution of 10 mM NBD' in acetonitrile (MeCN) (Sigma-Aldrich, 99.999%) was used. Additionally, 0.1 M tetrabutylammoniumperchlorate (TBAP) (Sigma Aldrich 99.0%) was used as supporting electrolyte in the measurements with an external potential applied. Potential control was provided by a commercial potentiostat (Gamry, Reference 600) using a three-electrode configuration with a graphite rod as counter electrode and an $Ag/Ag^+$ electrode (0.01 M $AgNO_3$ with 0.1 M TBAP in MeCN) as reference electrode (RE). The calibration of the RE was performed in an external cell versus the cyclic voltammogram of ferrocene (Alfa Aesar, 99.5%). Note, that in this work all potentials are referred to the redox potential of the ferrocene couple ($V_{fc}$).

**STM:** To ensure a clean and defect-free surface, the Au(111) crystal was initially annealed by inductive heating (Ambrell, EasyHeat) at 873 – 1073 K for 45 min. Subsequently, we irradiated the Au(111) sample in a solution of 10 mM NBD' in MeCN at OCP for 60 min in the PEC-IRRAS setup described above. As reference experiment we performed the same procedure in the absence of NBD'. After the treatment, the Au(111) crystal was carefully rinsed with MeCN and directly transferred to the STM setup. We used a commercial STM/AFM system (Keysight Technologies, Series 5500 AFM/SPM) equipped with a combination of active and passive noise damping. The STM tips were mechanically cut from a PtIr (80:20) wire (MaTecK, 99.99%, d = 0.25 mm). The STM images were obtained in constant current mode with a current of 0.1 nA and with a bias voltage of 0.2 V applied to the sample. The STM images were post-processed (row-aligning, data leveling) using the Gwyddion software (version 2.53).[51]

**Acknowledgements**

The authors acknowledge financial support by the Deutsche Forschungsgemeinschaft (DFG) (392607742) and additional support by the DFG (Collaborative Research Centre SFB 1452 – Catalysis at Liquid Interfaces, Research Unit FOR 1878 "Functional Molecular Structures on Complex Oxide Surfaces", projects 214951840, 322419553). We thank Andreas Leng and Andreas Hirsch for their contributions to the quantitative analysis and Lukas Fromm and Andreas Görling for estimating the particle radius of the NBD'. KMP acknowledges support from the Swedish Research Council FORMAS, the Swedish Energy Agency and European Union's Horizon 2020 Framework Programme under grant agreement number 951801 for financial support.

**Supporting Information**

Time resolved spectra of the NBD'/QC' system during irradiation and back-conversion at -0.7 $V_{fc}$ and band assignment; Details on the quantitative analysis of the IR spectra; Model for the kinetic evaluation of the system; Potential dependent $k_s$ values and $k_s$ values over 1000 cycles; Determination of the sensitivity limit of the experiment over 1000 cycles; Reversibility test of the catalytically triggered NBD'-QC' energy storage system on Au(111) in MeCN over 1000 cycles. Comparison of the catalytic activity of Au(111) with Pt(111). Differentiation between catalytic and electrochemical reaction channel. Stability of QC' under reductive potentials.

The Supporting Information is available free of charge on the ACS Publications website.

**References**


1. Kucharski, T. J.; Ferralis, N.; Kolpak, A. M.; Zheng, J. O.; Nocera, D. G.; Grossman, J. C., Templated assembly of photoswitches significantly increases the energy-storage capacity of solar thermal fuels. *Nature Chemistry* **2014,** *6* (5), 441-447.
2. Kucharski, T. J.; Tian, Y.; Akbulatov, S.; Boulatov, R., Chemical solutions for the closed-cycle storage of solar energy. *Energy & Environmental Science* **2011,** *4* (11), 4449-4472.
3. Lennartson, A.; Moth-Poulsen, K., Molecular Solar-Thermal Energy Storage: Molecular Design and Functional Devices. In *Molecular Devices for Solar Energy Conversion and Storage*, Tian, H.; Boschloo, G.; Hagfeldt, A., Eds. Springer Singapore: Singapore, 2018; pp 327-352.
4. Wang, Z.; Erhart, P.; Li, T.; Zhang, Z.-Y.; Sampedro, D.; Hu, Z.; Wegner, H. A.; Brummel, O.; Libuda, J.; Nielsen, M. B.; Moth-Poulsen, K., Storing energy with molecular photoisomers. *Joule* **2021,** *5* (12), 3116-3136.
5. Moth-Poulsen, K.; Coso, D.; Borjesson, K.; Vinokurov, N.; Meier, S. K.; Majumdar, A.; Vollhardt, K. P. C.; Segalman, R. A., Molecular solar thermal (MOST) energy storage and release system. *Energy & Environmental Science* **2012,** *5* (9), 8534-8537.
6. Waldeck, D. H., Photoisomerization dynamics of stilbenes. *Chemical Reviews* **1991,** *91* (3), 415-436.
7. Lennartson, A.; Roffey, A.; Moth-Poulsen, K., Designing photoswitches for molecular solar thermal energy storage. *Tetrahedron letters* **2015,** *56* (12), 1457-1465.
8. Han, G. G. D.; Li, H.; Grossman, J. C., Optically-controlled long-term storage and release of thermal energy in phase-change materials. *Nature Communications* **2017,** *8* (1), 1446.
9. Beharry, A. A.; Woolley, G. A., Azobenzene photoswitches for biomolecules. *Chemical Society Reviews* **2011,** *40* (8), 4422-4437.
10. Mogensen, J.; Christensen, O.; Kilde, M. D.; Abildgaard, M.; Metz, L.; Kadziola, A.; Jevric, M.; Mikkelsen, K. V.; Nielsen, M. B., Molecular Solar Thermal Energy Storage Systems with Long Discharge Times Based on the Dihydroazulene/Vinylheptafulvene Couple. *European Journal of Organic Chemistry* **2019,** *2019* (10), 1986-1993.
11. Brough, S. A.; Lamm, A. N.; Liu, S.-Y.; Bettinger, H. F., Photoisomerization of 1,2-Dihydro-1,2-Azaborine: A Matrix Isolation Study. *Angewandte Chemie International Edition* **2012,** *51* (43), 10880-10883.
12. Cristol, S. J.; Snell, R. L., Bridged Polycyclic Compounds. VI. The Photoisomerization of Bicyclo [2,2,1]hepta-2,5-diene-2,3-dicarboxylic Acid to Quadricyclo [2,2,1,02,6,03,5]heptane-2,3-dicarboxylic Acid1,2. *Journal of the American Chemical Society* **1958,** *80* (8), 1950-1952.
13. Schwarz, M.; Schuschke, C.; Silva, T. N.; Mohr, S.; Waidhas, F.; Brummel, O.; Libuda, J., A Simple High-Intensity UV-Photon Source for Photochemical Studies in UHV: Application to the Photoconversion of Norbornadiene to Quadricyclane *Review of Scientific Instruments* **2019,** *90* (2), 024105.
14. Schwendiman, D. P.; Kutal, C., Transition Metal Photoassisted Valence Isomerization of Norbornadiene. An Attractive Energy-Storage Reaction. *Inorganic Chemistry* **1977,** *16* (3), 719-721.
15. Bauer, U.; Mohr, S.; Döpper, T.; Bachmann, P.; Späth, F.; Düll, F.; Schwarz, M.; Brummel, O.; Fromm, L.; Pinkert, U.; Görling, A.; Hirsch, A.; Bachmann, J.; Steinrück, H.-P.; Libuda, J.; Papp, C., Catalytically Triggered Energy Release from Strained Organic Molecules: The Surface Chemistry of Quadricyclane and Norbornadiene on Pt(111). *Chemistry – A European Journal* **2017,** *23* (7), 1613-1622.

16. Bertram, M.; Waidhas, F.; Jevric, M.; Fromm, L.; Schuschke, C.; Kastenmeier, M.; Görling, A.; Moth-Poulsen, K.; Brummel, O.; Libuda, J., Norbornadiene photoswitches anchored to well-defined oxide surfaces: From ultrahigh vacuum into the liquid and the electrochemical environment. *The Journal of Chemical Physics* **2020,** *152* (4), 044708.
17. Dreos, A.; Wang, Z.; Tebikachew, B. E.; Moth-Poulsen, K.; Andréasson, J., Three-Input Molecular Keypad Lock Based on a Norbornadiene–Quadricyclane Photoswitch. *The Journal of Physical Chemistry Letters* **2018,** *9* (21), 6174-6178.
18. Quant, M.; Hamrin, A.; Lennartson, A.; Erhart, P.; Moth-Poulsen, K., Solvent Effects on the Absorption Profile, Kinetic Stability, and Photoisomerization Process of the Norbornadiene–Quadricyclanes System. *The Journal of Physical Chemistry C* **2019,** *123* (12), 7081-7087.
19. Mansø, M.; Kilde, M. D.; Singh, S. K.; Erhart, P.; Moth-Poulsen, K.; Nielsen, M. B., Dithiafulvene derivatized donor–acceptor norbornadienes with redshifted absorption. *Physical Chemistry Chemical Physics* **2019,** *21* (6), 3092-3097.
20. Kazuhiro, M.; Kazutoshi, T.; Yoshinori, N.; Yoshinori, Y., Photoisomerization of Norbornadiene to Quadricyclane in the Presence of Copper(I)-Nitrogen Ligand Catalysts. *Chemistry Letters* **1980,** *9* (10), 1259-1262.
21. Liu, Y.-T.; Liu, S.; Li, G.-R.; Gao, X.-P., Strategy of Enhancing the Volumetric Energy Density for Lithium–Sulfur Batteries. *Advanced Materials* **2021,** *33* (8), 2003955.
22. Wang, Z.; Roffey, A.; Losantos, R.; Lennartson, A.; Jevric, M.; Petersen, A. U.; Quant, M.; Dreos, A.; Wen, X.; Sampedro, D.; Börjesson, K.; Moth-Poulsen, K., Macroscopic heat release in a molecular solar thermal energy storage system. *Energy & Environmental Science* **2019**.
23. Dreos, A.; Börjesson, K.; Wang, Z.; Roffey, A.; Norwood, Z.; Kushnir, D.; Moth-Poulsen, K., Exploring the potential of a hybrid device combining solar water heating and molecular solar thermal energy storage. *Energy & Environmental Science* **2017,** *10* (3), 728-734.
24. Kashyap, V.; Sakunkaewkasem, S.; Jafari, P.; Nazari, M.; Eslami, B.; Nazifi, S.; Irajizad, P.; Marquez, M. D.; Lee, T. R.; Ghasemi, H., Full Spectrum Solar Thermal Energy Harvesting and Storage by a Molecular and Phase-Change Hybrid Material. *Joule* **2019,** *3* (12), 3100-3111.
25. Wang, Z.; Wu, Z.; Hu, Z.; Orrego-Hernández, J.; Mu, E.; Zhang, Z.-Y.; Jevric, M.; Liu, Y.; Fu, X.; Wang, F.; Li, T.; Moth-Poulsen, K., Chip-scale solar thermal electrical power generation. *Cell Reports Physical Science* **2022,** *3* (3), 100789.
26. Wang, Z.; Hölzel, H.; Moth-Poulsen, K., Status and Challenges for Molecular Solar Thermal Energy Storage System Based Devices. under review.
27. Cuppoletti, A.; Dinnocenzo, J. P.; Goodman, J. L.; Gould, I. R., Bond-Coupled Electron Transfer Reactions: Photoisomerization of Norbornadiene to Quadricyclane. *The Journal of Physical Chemistry A* **1999,** *103* (51), 11253-11256.
28. Bren, V. A.; Dubonosov, A. D.; Minkin, V. I.; Chernoivanov, V. A., Norbornadiene–Quadricyclane — An Effective Molecular System for the Storage of Solar Energy. *Russian Chemical Reviews* **1991,** *60* (451).
29. Brummel, O.; Waidhas, F.; Bauer, U.; Wu, Y.; Bochmann, S.; Steinrück, H.-P.; Papp, C.; Bachmann, J.; Libuda, J., Photochemical Energy Storage and Electrochemically Triggered Energy Release in the Norbornadiene–Quadricyclane System: UV Photochemistry and IR Spectroelectrochemistry in a Combined Experiment. *The Journal of Physical Chemistry Letters* **2017,** *8* (13), 2819-2825.

30. M. Quant, A. Lennartson, A. Dreos, M. Kuisma, P. Erhart, K. Börjesson, K. Moth-Poulsen, Low Molecular Weight Norbornadiene Derivatives for Molecular Solar-Thermal Energy Storage. *Chemistry–A European Journal* **2016,** *22* (37), 13265-13274.
31. Jevric, M.; Petersen, A. U.; Mansø, M.; Kumar Singh, S.; Wang, Z.; Dreos, A.; Sumby, C.; Nielsen, M. B.; Börjesson, K.; Erhart, P.; Moth-Poulsen, K., Norbornadiene-Based Photoswitches with Exceptional Combination of Solar Spectrum Match and Long-Term Energy Storage. *Chemistry – A European Journal* **2018,** *24* (49), 12767-12772.
32. Hoffmann, R. W.; Barth, W., ECE-catalysed isomerisation of quadricyclanes. *Journal of the Chemical Society, Chemical Communications* **1983,** (7), 345-346.
33. Koser, G. F.; Faircloth, J. N., Silver (I)-Promoted Reactions of Strained Hydrocarbons. Oxidation vs. Rearrangement. *The Journal of Organic Chemistry* **1976,** *41* (3), 583-585.
34. Maruyama, K.; Tamiaki, H., Catalytic isomerization of water-soluble quadricyclane to norbornadiene derivatives induced by cobalt-porphyrin complexes. *The Journal of Organic Chemistry* **1986,** *51* (5), 602-606.
35. Wang, Z.; Roffey, A.; Losantos, R.; Lennartson, A.; Jevric, M.; Petersen, A. U.; Quant, M.; Dreos, A.; Wen, X.; Sampedro, D.; Börjesson, K.; Moth-Poulsen, K., Macroscopic Heat Release in a Molecular Solar Thermal Energy Storage System. *Energy and Environmental Science* **2019,** *12* (1), 187-193.
36. Sadao, M.; Yoshinobu, A.; Masayoshi, M.; Toshinobu, O.; Zen-ichi, Y.; Toshiro, M.; Masahiro, F.; Tomoaki, T., Alumina-Anchored Cobalt Porphine Catalysts for the Conversion of Quadricyclane to Norbornadiene. *Bulletin of the Chemical Society of Japan* **1988,** *61* (3), 973-981.
37. Fife, D. J.; Morse, K. W.; Moore, W. M., Thermal isomerization of quadricyclane to norbornadiene catalyzed by copper(II) and tin(II) salts. *Journal of the American Chemical Society* **1983,** *105* (25), 7404-7407.
38. Hirao, K.-i.; Yamashita, A.; Yonemitsu, O., Cycloreversion of acylquadricyclane to acylnorbornadiene promoted by metal oxides. *Tetrahedron Letters* **1988,** *29* (33), 4109-4112.
39. Luchs, T.; Lorenz, P.; Hirsch, A., Efficient Cyclization of the Norbornadiene-Quadricyclane Interconversion Mediated by a Magnetic [$Fe_3O_4$−CoSalphen] Nanoparticle Catalyst. *ChemPhotoChem* **2020,** *4* (1), 52-58.
40. Browne, W. R.; Kudernac, T.; Katsonis, N.; Areephong, J.; Hjelm, J.; Feringa, B. L., Electro-and photochemical switching of dithienylethene self-assembled monolayers on gold electrodes. *The Journal of Physical Chemistry C* **2008,** *112* (4), 1183-1190.
41. He, J.; Chen, F.; Liddell, P. A.; Andréasson, J.; Straight, S. D.; Gust, D.; Moore, T. A.; Moore, A. L.; Li, J.; Sankey, O. F., Switching of a photochromic molecule on gold electrodes: single-molecule measurements. *Nanotechnology* **2005,** *16* (6), 695.
42. Schlimm, A.; Löw, R.; Rusch, T.; Röhricht, F.; Strunskus, T.; Tellkamp, T.; Sönnichsen, F.; Manthe, U.; Magnussen, O.; Tuczek, F.; Herges, R., Long-Distance Rate Acceleration by Bulk Gold. *Angewandte Chemie International Edition* **2019,** *58* (20), 6574-6578.
43. Löw, R.; Rusch, T.; Moje, T.; Röhricht, F.; Magnussen, O. M.; Herges, R., Norbornadiene-functionalized triazatriangulenium and trioxatriangulenium platforms. *Beilstein Journal of Organic Chemistry* **2019,** *15*, 1815-1821.
44. Eschenbacher, R.; Xu, T.; Franz, E.; Löw, R.; Moje, T.; Fromm, L.; Görling, A.; Brummel, O.; Herges, R.; Libuda, J., Triggering the energy release in molecular solar thermal

systems: Norbornadiene-functionalized trioxatriangulen on Au(111). *Nano Energy* **2022,** *95*, 107007.
45. U. Bauer, L. Fromm, C. Weiß, P. Bachmann, F. Späth, F. Düll, J. Steinhauer, W. Hieringer, A. Görling, A. Hirsch, Controlled Catalytic Energy Release of the Norbornadiene/Quadricyclane Molecular Solar Thermal Energy Storage System on Ni (111). *The Journal of Physical Chemistry C* **2018,** *123* (13), 7654-7664.
46. Brummel, O.; Besold, D.; Döpper, T.; Wu, Y.; Bochmann, S.; Lazzari, F.; Waidhas, F.; Bauer, U.; Bachmann, P.; Papp, C.; Steinrück, H.-P.; Görling, A.; Libuda, J.; Bachmann, J., Energy Storage in Strained Organic Molecules: (Spectro)Electrochemical Characterization of Norbornadiene and Quadricyclane. *ChemSusChem* **2016,** *9* (12), 1424-1432.
47. Waidhas, F.; Jevric, M.; Fromm, L.; Bertram, M.; Görling, A.; Moth-Poulsen, K.; Brummel, O.; Libuda, J., Electrochemically controlled energy storage in a norbornadiene-based solar fuel with 99% reversibility. *Nano Energy* **2019,** *63*, 103872.
48. Waidhas, F.; Jevric, M.; Bosch, M.; Yang, T.; Franz, E.; Liu, Z.; Bachmann, J.; Moth-Poulsen, K.; Brummel, O.; Libuda, J., Electrochemically Controlled Energy Release from a Norbornadiene-Based Solar Thermal Fuel: Increasing the Reversibility to 99.8% using HOPG as the Electrode Material. *Journal of Materials Chemistry A* **2020,** *8* (31), 15658–15664.
49. Jevric, M.; Petersen, A. U.; Mansø, M.; Kumar Singh, S.; Wang, Z.; Dreos, A.; Sumby, C.; Nielsen, M. B.; Börjesson, K.; Erhart, P.; Moth-Poulsen, K., Norbornadiene-Based Photoswitches with Exceptional Combination of Solar Spectrum Match and Long-Term Energy Storage. *Chemistry – A European Journal* **2018,** *24* (49), 12767-12772.
50. Faisal, F.; Bertram, M.; Stumm, C.; Waidhas, F.; Brummel, O.; Libuda, J., Preparation of complex model electrocatalysts in ultra-high vacuum and transfer into the electrolyte for electrochemical IR spectroscopy and other techniques. *Review of Scientific Instruments* **2018,** *89* (11), 114101.
51. Nečas, D.; Klapetek, P., Gwyddion: an open-source software for SPM data analysis. *Open Physics* **2012,** *10* (1), 181.

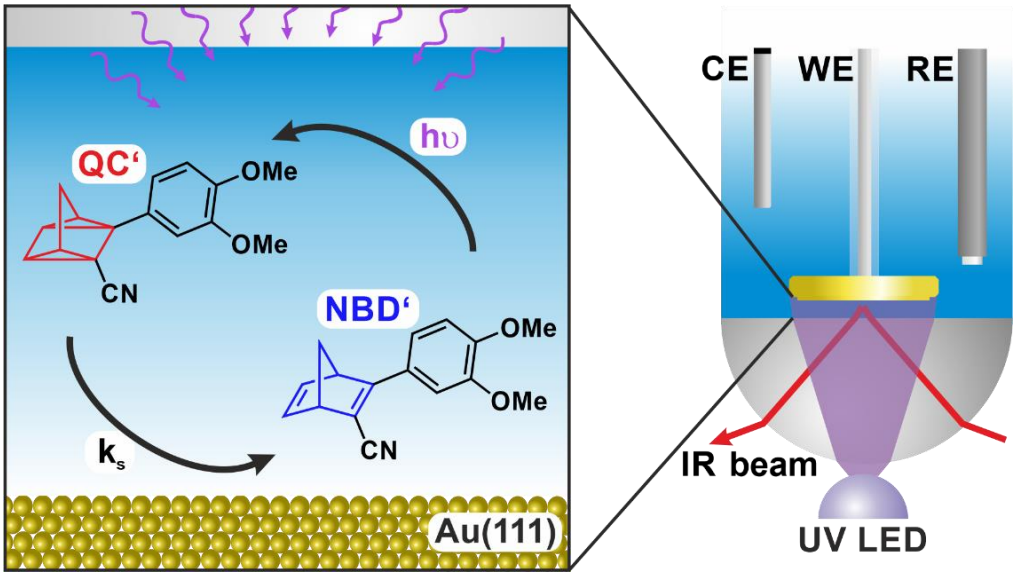


**Figure 1:** MOST/catalyst system and experimental setup. (left) Schematic representation of the energy storage and release process for the MOST system 2-cyano-3-(3,4-dimethoxyphenyl)-norbornadiene (NBD') and 2-cyano-3-(3,4-dimethoxyphenyl)-quadricyclane (QC'). (right) Schematic representation of the PEC-IRRAS experiment (CE, counter electrode; WE working electrode; RE reference electrode).

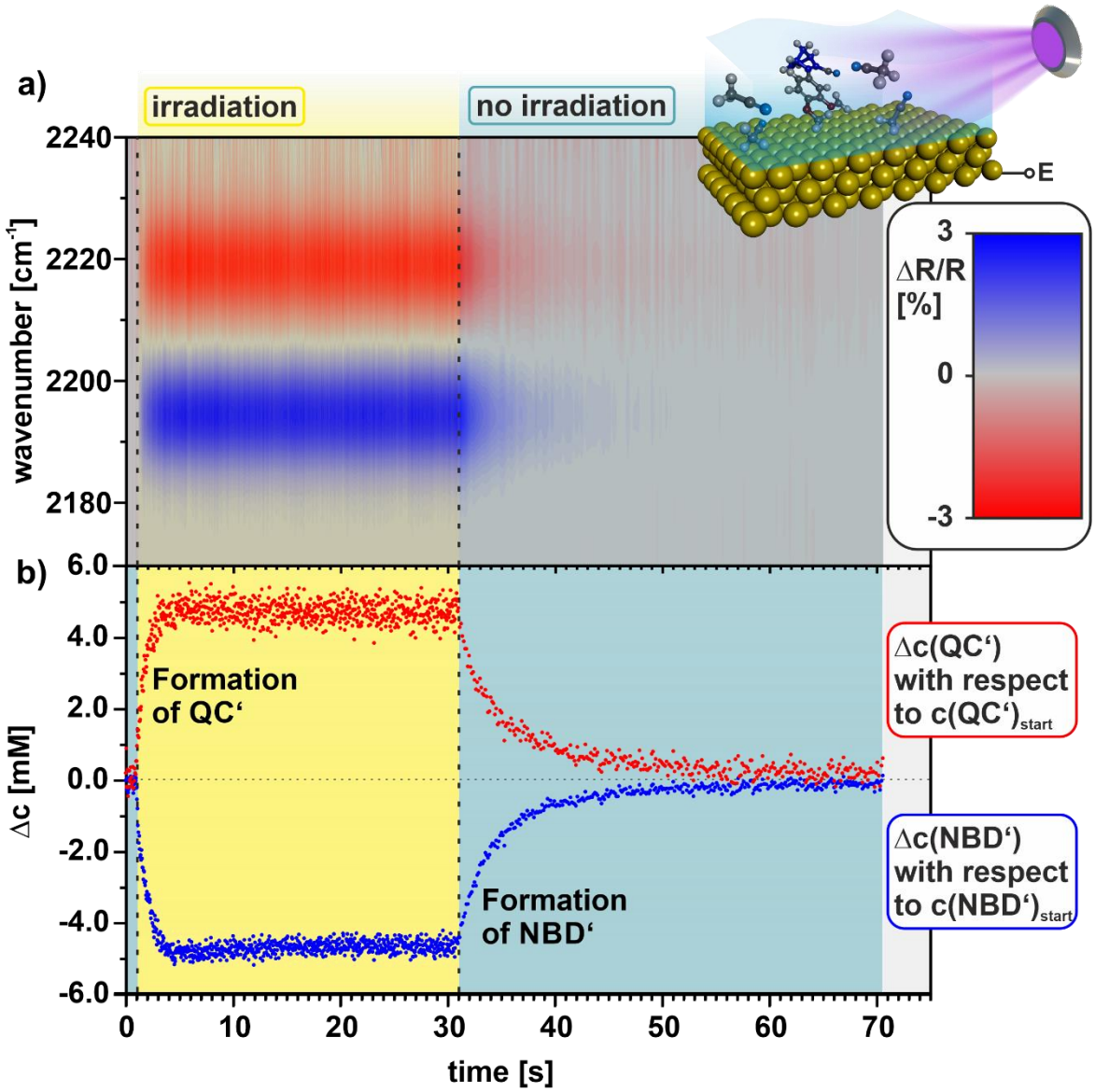


**Figure 2:** Photochemical conversion and catalytically triggered back-conversion in the NBD'/QC' system. a) Color plot of the ν(CN) region of the IR spectra during irradiation and catalytically triggered back-conversion; b) Relative change of concentration of NBD' and QC' during irradiation and catalytically triggered back-conversion; all spectra were acquired with 10 mM NBD' in MeCN at -0.7 $V_{fc}$.

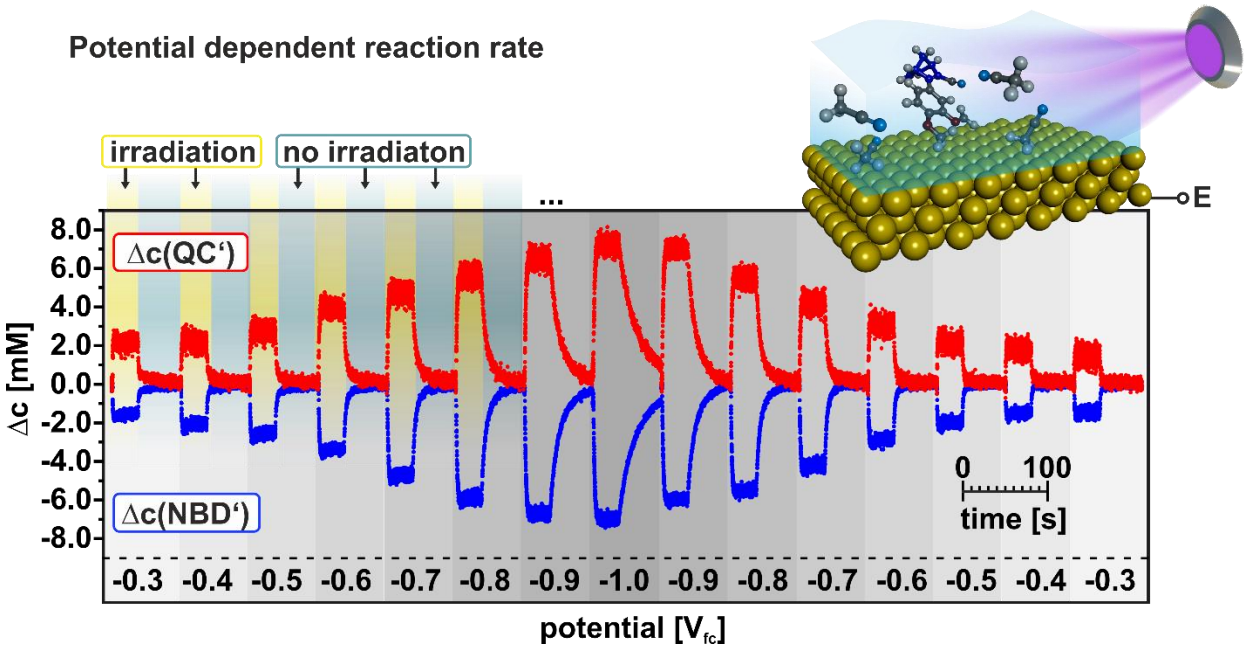


**Figure 3:** Change of concentrations during photochemical conversion and catalytically triggered back-conversion in the NBD'/QC' system at different potentials of the Au(111) electrode between -0.3 $V_{fc}$ and -1.0 $V_{fc}$.

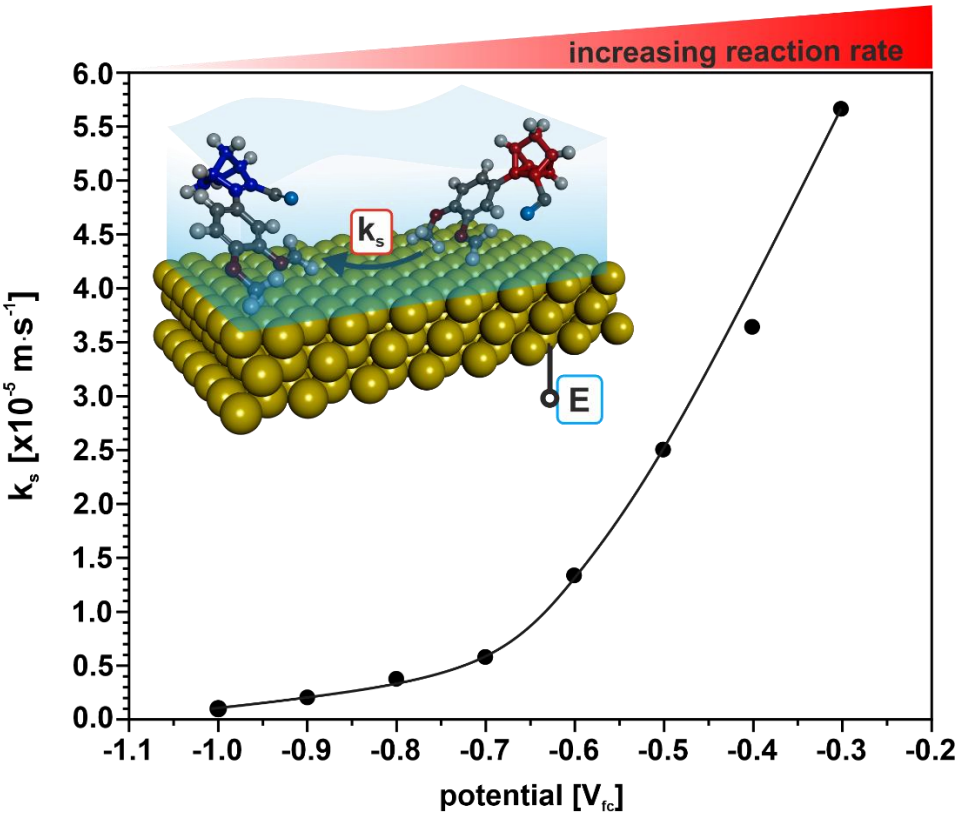


**Figure 4:** Values of the rate-constant $k_s$ for the catalytically triggered back-reaction as a function of the potential applied to the Au electrode (see Supporting Information for details of the kinetic model).

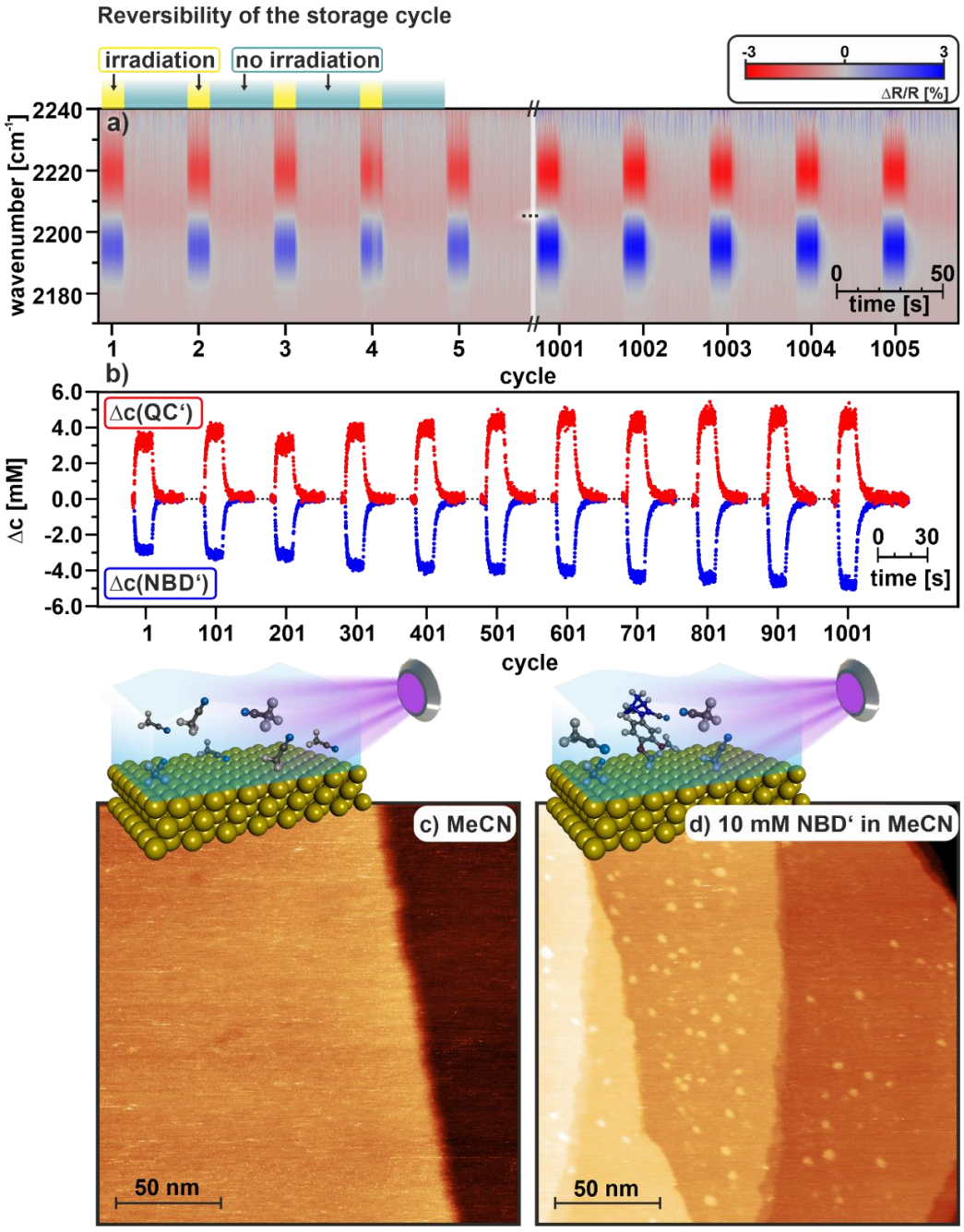


**Figure 5:** Stability of the NBD'-QC'/Au(111) system probed over 1000 storage and release cycles (between steady-state and total back-conversion); a) Color plot of the ν(CN) region of the IR spectra recorded during selected energy storage and release cycles; b) change of the concentrations of QC' and NBD' for selected storage and release cycles. All spectra were acquired in MeCN at -0.7 $V_{fc}$; c) and d) STM image of the Au(111) surface after 60 min continuous irradiation at OCP in c) MeCN and d) 10 mM NBD' in MeCN.